Inorganic Chemistry

Article

pubs.acs.org/IC

Syntheses, Structures, and Magnetic Properties of a Family of Tetranuclear Hydroxido-Bridged $Ni^{II}_2Ln^{III}_2$ (Ln = La, Gd, Tb, and Dy) Complexes: Display of Slow Magnetic Relaxation by the Zinc(II)–Dysprosium(III) Analogue

Sk Md Towsif Abtab,[†] Manoranjan Maity,[†] Kisholoy Bhattacharya,[†] E. Carolina Sañudo,[‡] and Muktimoy Chaudhury*,[†]

[†]Department of Inorganic Chemistry, Indian Association for the Cultivation of Science, Kolkata 700 032, India

[‡]Departament de Química Inorgànica i Institut de Nanociència i Nanotecnologia, Universitat de Barcelona, Diagonal 645, 08028 Barcelona, Spain

Supporting Information

ABSTRACT: A new family of [2 × 2] tetranuclear 3d–4f heterometallic complexes have been synthesized. These are $[Zn_2Dy_2L_2(\mu_3\text{-}OH)_2(\mu_4\text{-}OH)(dbm)_2(MeOH)_2](NO_3)\cdot 2H_2O\cdot MeOH$ (**3**), $[Ni_2Dy_2L_2(\mu_3\text{-}OH)_2(\mu_4\text{-}OH)(dbm)_2(MeOH)_2](NO_3)\cdot MeOH$ (**4**), $[Ni_2La_2L_2(\mu_3\text{-}OH)_2(\mu_4\text{-}OH)(dbm)_2(MeOH)_2](ClO_4)\cdot H_2O\cdot 2MeOH$ (**5**), $[Ni_2Tb_2L_2(\mu_3\text{-}OH)_2(\mu_4\text{-}OH)(dbm)_2(MeOH)_2](NO_3)\cdot MeOH$ (**6**), and $[Ni_2Gd_2L_2(\mu_3\text{-}OH)_2(\mu_4\text{-}OH)(dbm)_2(MeOH)_2](NO_3)\cdot MeOH$ (**7**), [H_2L = *N*,*N*′-dimethyl-*N*,*N*′-bis(2-hydroxy-3,5-dimethylbenzyl)ethylenediamine and Hdbm = dibenzoylmethane] obtained through a single-pot synthesis using [Zn(HL)(dbm)] (for **3**)/[Ni(HL)(dbm)]·2CH_3OH (for **4**, **5**, **6**, and **7**) as 3d-metal ion precursors. Single-crystal X-ray diffraction analysis and electrospray ionization (ESI) mass spectroscopy have been used to establish their identities. Compounds are isostructural, in which the metal ions are all connected together by a bridging hydroxido ligand in a rare μ_4-mode. In complexes **3**–**7**, the metal ions are antiferromagnetically coupled. Taking a cue from the results of **3** and **5**, precise estimations have been made for the antiferromagnetic Ni···Ni (J_{Ni} = −50 cm^{-1}), Ni···Gd (J_{NiGd} = −4.65 cm^{-1}), and Gd···Gd (J_{Gd} = −0.02 cm^{-1}) exchange interactions in **7**, involving the gadolinium(III) ions. The $Zn^{II}_2Dy^{III}_2$ compound **3** has shown the tail of an out-of-phase signal in alternating current (AC) susceptibility measurement, indicative of slow relaxation of magnetization. Interestingly, the $Ni^{II}_2Dy^{III}_2$ compound **4** in which both the participating metal ions possess large single ion anisotropy, has failed to show up any slow magnetic relaxation.

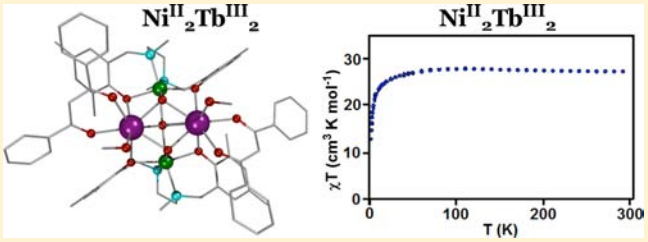

INTRODUCTION

The design and synthesis of heterometal complexes containing both 3d and 4f metal ions have attracted increasing attention because of their potential applications in numerous areas including manufacture of light conversion devices,[1] coordination polymers,[2] electrochemical, and bimetallic catalysis,[3,4] and in molecular magnetism.[5] Since the first discovery of single-molecule magnet (SMM) in a Mn_{12} cluster, much effort has been focused on the preparation of new molecular aggregates possessing simultaneously a high-spin ground state and a large easy-axis type magnetic anisotropy.[6] More recently, the strategy of combining 3d and 4f metal ions has successfully led to several Mn/Ln,[7] Fe/Ln,[8] Co/Ln,[9] Ni/Ln,[10] Cu/Ln,[11] and Zn/Ln[12] SMMs. In this context, Tb^{III}, Dy^{III}, and Ho^{III} ions which possess significant single-ion magnetic anisotropy arising from their large unquenched orbital angular momentum as well as several unpaired electrons are appearing to be highly promising.[5a] It is of interest for coordination chemists to prepare new 3d–4f heterometal complexes to generate more information for magneto-structural correlation, thus further enriching the SMM family.

As a part of our ongoing program on the development of convenient synthetic protocols for 3d–4f complexes, we have been interested to explore the possibility of obtaining Ln^{III}-Ni^{II} heterometal complexes as possible SMMs taking advantage of the nickel(II) ion's significantly large single-ion anisotropy[13] and noting that terbium(III), dysprosium(III), and holmium(III) show interesting magnetic behavior because of their large unquenched orbital angular momentum associated with the internal nature of the valence f orbitals.[14] Herein, we describe the syntheses of a new family of 3d–4f tetranuclear $Ni^{II}_2Ln^{III}_2$ complexes obtained via "metal complexes as ligand" approach. These complexes, namely, $[Zn_2Dy_2L_2(\mu_3\text{-}OH)_2(\mu_4\text{-}OH)(dbm)_2(MeOH)_2](NO_3)\cdot 2H_2O\cdot MeOH$ (**3**), $[Ni_2Dy_2L_2(\mu_3\text{-}OH)_2(\mu_4\text{-}OH)(dbm)_2(MeOH)_2](NO_3)\cdot MeOH$ (**4**),

Received: May 30, 2012
Published: September 20, 2012

   dx.doi.org/10.1021/ic301138r | *Inorg. Chem.* 2012, 51, 10211–10221

$[Ni_2La_2L_2(\mu_3\text{-}OH)_2(\mu_4\text{-}OH)(dbm)_2(MeOH)_2]\text{-}(ClO_4)\cdot H_2O\cdot 2MeOH$ (**5**), $[Ni_2Tb_2L_2(\mu_3\text{-}OH)_2(\mu_4\text{-}OH)\text{-}(dbm)_2(MeOH)_2](NO_3)$ MeOH (**6**), and $[Ni_2Gd_2L_2(\mu_3\text{-}OH)_2(\mu_4\text{-}OH)(dbm)_2(MeOH)_2](NO_3)\cdot$MeOH (**7**), [$H_2L$ = *N,N′*-dimethyl-*N,N′*-bis(2-hydroxy-3,5-dimethylbenzyl) ethylenediamine and Hdbm = dibenzoylmethane] are obtained through single pot synthesis using [Zn(HL)(dbm)] (for **3**)/ $[Ni(HL)(dbm)]\cdot 2CH_3OH$ (for **4**, **5**, **6**, and **7**) as 3d-metal ion precursors. Their characterizations and magnetic properties are reported in details.

EXPERIMENTAL SECTION

Materials. The tetradentate ligand *N,N′*-dimethyl-*N,N′*-bis(2-hydroxy-3,5-dimethylbenzyl)ethylenediamine (H_2L) was prepared according to a reported method.[15] All other reagents were obtained from commercial sources and used as received. All reactions were carried out under aerobic conditions. Solvents were reagent grade, dried by standard methods,[16] and distilled under nitrogen prior to their use.

Preparation of Compounds. $[Ni(HL)(dbm)]\cdot 2CH_3OH$ (1). Nickel(II) perchlorate hexahydrate (0.36 g, 1 mmol) and H_2L (0.36 g, 1 mmol) were dissolved in methanol (30 mL). Dibenzoylmethane (0.22 g, 1 mmol) in solid was added to the resulting green solution. Triethylamine (0.20 g, 2 mmol) was then added, and the resulting solution was stirred for about 2 h at ambient temperature when a green microcrystalline compound was separated. It was collected by filtration and recrystallized from methanol/acetone solvent mixture. Some of these crystals were of diffraction grade and used directly for X-ray crystallographic analysis. Yield: 0.56 g (80%). Anal. Calcd for $C_{39}H_{50}N_2NiO_6$: C, 66.76; H, 7.19; N, 3.99. Found: C, 66.62; H, 7.14; N, 4.02%. FT-IR bands (KBr pellet, cm^{-1}): 2974, 2902, 2855, 1600, 1558, 1518, 1476, 1464, 1411, 1313, 1272, 1223, 1157, 1050, 1025, 860, 755, 721, 688, 629, 524.

[Zn(HL)(dbm)] (2). This compound was prepared following a similar procedure as described for **1**, except that $Zn(ClO_4)_2\cdot 6H_2O$ was used instead of $Ni(ClO_4)_2\cdot 6H_2O$. The resulting yellow solution was allowed to stand in the air for slow evaporation. Yellow microcrystalline compound formed in about one week time was collected by filtration and dried over fused $CaCl_2$. X-ray diffraction quality crystals were obtained by recrystallization from a mixture of acetone and methanol. Yield: 0.46 g (72%). Anal. Calcd for $C_{37}H_{42}N_2O_4Zn$: C, 68.97; H, 6.58; N, 4.35. Found: C, 68.84; H, 6.53; N, 4.38%. FT-IR bands (KBr pellet, cm^{-1}): 2999, 2904, 1598, 1556, 1517, 1477, 1456, 1400, 1311, 1251, 1224, 1157, 1078, 1024, 860, 786, 755, 723, 690, 621.

$[Zn_2Dy_2L_2(\mu_3\text{-}OH)_2(\mu_4\text{-}OH)(dbm)_2(MeOH)_2](NO_3)\cdot 2H_2O\cdot$MeOH (3). To a stirred methanolic solution (20 mL) of $Dy(NO_3)_3\cdot 6H_2O$ (0.046 g, 0.1 mmol) was added **2** (0.065 g, 0.1 mmol) in solid form. Tetrabutylammonium hydroxide solution (40 wt % in water, 0.13 g, 0.2 mmol) was then added to the resulting yellow solution and refluxed for 15 min. The solution was cooled to room temperature, filtered, and the filtrate was reduced to about 5 mL volume by rotary evaporation. Dichloromethane (5 mL) was then added to it, and the solution was allowed to evaporate slowly at room temperature. Yellow crystals, suitable for single-crystal X-ray diffraction analysis, were obtained after 3−4 days. Yield: 0.055 g (59%). Anal. Calcd for $C_{77}H_{101}Dy_2N_5O_{19}Zn_2$: C, 49.80; H, 5.49; N, 3.77. Found: C, 49.68; H, 5.46; N, 3.80%. FT-IR bands (KBr pellet, cm^{-1}): 3061, 2999, 2958, 2912, 2860, 2816, 1599, 1552, 1518, 1479, 1454, 1390, 1307, 1259, 1226, 1182, 1159, 1070, 1026, 999, 945, 858, 806, 783, 752, 723, 690, 611, 524, 519.

$[Ni_2Dy_2L_2(\mu_3\text{-}OH)_2(\mu_4\text{-}OH)(dbm)_2(MeOH)_2](NO_3)\cdot$MeOH (4). $Dy(NO_3)_3\cdot 6H_2O$ (0.046 g, 0.1 mmol) was added to a slurry of **1** (0.070 g, 0.1 mmol) in methanol (10 mL) at ambient temperature under stirring condition. To the resulting green solution, tetrabutylammonium hydroxide (40 wt % in water, 0.13 g, 0.2 mmol) was added and refluxed for 20 min. The resulting solution was allowed to stand for an overnight period to get the crystalline product. Single crystals suitable for X-ray structure analysis were obtained by the diffusion of dichloromethane into a methanolic solution of the compound. Yield: 0.062 g (68%). Anal. Calcd for $C_{77}H_{97}Dy_2N_5Ni_2O_{17}$: C, 51.16; H, 5.41; N, 3.88. Found: C, 51.23; H, 5.45; N, 3.91%. FT-IR bands (KBr pellet, cm^{-1}): 3061, 2966, 2916, 2862, 2816, 1597, 1550, 1519, 1479, 1454, 1392, 1369, 1307, 1261, 1225, 1182, 1120, 1070, 1026, 999, 945, 858, 808, 783, 750, 721, 690, 613, 524. ESI-MS (positive ion mode) in CH_3CN: m/z 1648 $[M\text{-}NO_3\text{-}3CH_3OH]^+$.

$[Ni_2La_2L_2(\mu_3\text{-}OH)_2(\mu_4\text{-}OH)(dbm)_2(MeOH)_2](ClO_4)\cdot H_2O\cdot 2$MeOH (5). This compound was prepared using the same procedure as that described above for the synthesis of its dysprosium(III) cognate **4** but using $La(ClO_4)_3\cdot 6H_2O$ in place of $Dy(NO_3)_3\cdot 6H_2O$. Yield: 0.060 g (65%). Anal. Calcd for $C_{78}H_{103}ClLa_2N_4Ni_2O_{20}$: C, 50.71; H, 5.62; N, 3.03. Found: C, 50.54; H, 5.59; N, 2.99%. FT-IR bands (KBr pellet, cm^{-1}): 3059, 2966, 2912, 2862, 2817, 1597, 1548, 1518, 1479, 1454, 1388, 1369, 1307, 1261, 1224, 1183, 1118, 1068, 1026, 997, 945, 860, 804, 783, 750, 721, 690, 623, 501, 497. ESI-MS (positive ion mode) in CH_3CN: m/z 1600 $[M\text{-}ClO_4\text{-}4CH_3OH\text{-}H_2O]^+$.

$[Ni_2Tb_2L_2(\mu_3\text{-}OH)_2(\mu_4\text{-}OH)(dbm)_2(MeOH)_2](NO_3)\cdot$MeOH (6). This compound was prepared following the same procedure as for **4**, using $Tb(NO_3)_3\cdot 6H_2O$ instead of $Dy(NO_3)_3\cdot 6H_2O$. Yield: 0.055 g (61%). Anal. Calcd for $C_{77}H_{97}N_5Ni_2O_{17}Tb_2$: C, 51.36; H, 5.43; N, 3.89. Found: C, 51.45; H, 5.40; N, 3.93%. FT-IR bands (KBr pellet, cm^{-1}): 3061, 2995, 2912, 2862, 2817, 1597, 1550, 1519, 1479, 1454, 1392, 1369, 1307, 1261, 1226, 1183, 1114, 1093, 1068, 1026, 1003, 943, 860, 808, 781, 752, 721, 690, 611, 528. ESI-MS (positive ion mode) in CH_3CN: m/z 1640 $[M\text{-}NO_3\text{-}3CH_3OH]^+$.

$[Ni_2Gd_2L_2(\mu_3\text{-}OH)_2(\mu_4\text{-}OH)(dbm)_2(MeOH)_2](NO_3)\cdot$MeOH (7). Compound **7** was prepared in the same way as for **4**, using $Gd(NO_3)_3\cdot 6H_2O$ instead of $Dy(NO_3)_3\cdot 6H_2O$ as the 4f metal ion source. The product obtained as a green crystalline solid was collected by filtration, washed with cold methanol, and dried in the air. We were unable to grow the diffraction grade crystals of this compound in spite of our repeated attempts. Yield: 0.063 g (70%). Anal. Calcd for $C_{77}H_{97}Gd_2N_5Ni_2O_{17}$: C, 51.46; H, 5.44; N, 3.90. Found: C, 51.32; H, 5.38; N, 3.98%. FT-IR bands (KBr pellet, cm^{-1}): 3431, 3061, 2995, 2914, 2860, 1599, 1550, 1520, 1477, 1454, 1392, 1307, 1261, 1226, 1117, 1093, 1068, 1026, 1003, 943, 860, 808, 780, 750, 723, 690, 615, 528. ESI-MS (positive ion mode) in CH_3CN: m/z 1637 $[M\text{-}NO_3\text{-}3CH_3OH]^+$.

Physical Measurements. Elemental (for C, H, and N) analyses were performed at IACS on a Perkin-Elmer model 2400 Series II CHNS Analyzer. IR spectra of the samples prepared as KBr pellets were recorded using a Shimadzu model 8400S FT-IR spectrometer. Electrospray ionization mass spectrometry (ESI-MS) spectra (in positive ion mode) were recorded on a QTOF model YA263 micromass spectrometer. A standard built-in software package, Masslynx. 4.0 supplied by Micromass, has been used for data simulation. Magnetic measurements were carried out on polycrystalline samples (about 30 mg) at the Serveis Científico-Tècnics of the Universitat de Barcelona (SPAIN) with a Quantum Design SQUID MPMS-XL magnetometer equipped with a 5 T magnet. Diamagnetic corrections were calculated using Pascal's constants and an experimental correction for the diamagnetic sample holder was applied.

X-ray Crystallography. Suitable single crystals of **3** (yellow block, $0.28 \times 0.22 \times 0.20$ mm^3), **4** (green block, $0.26 \times 0.22 \times 0.18$ mm^3), **5** (green block, $0.30 \times 0.26 \times 0.22$ mm^3), and **6** (green block, $0.27 \times 0.24 \times 0.20$ mm^3) were selected for single-crystal X-ray diffraction analysis and mounted on glass fibers. Intensity data for the compounds were measured employing a Bruker SMART APEX II CCD diffractometer equipped with a monochromatized Mo K_α radiation ($\lambda = 0.71073$ Å) source using the $\omega/2\theta$ scan technique at 298(2) K for all the complexes. No crystal decay was observed during the data collections. The intensity data were corrected for empirical absorption. In all cases, absorption corrections based on multiscan using the SADABS software[17] were applied.

The structures were solved by direct methods[18] and refined on F^2 by a full-matrix least-squares procedure[18] based on all data minimizing

Table 1. Summary of the Crystallographic Data for the Complexes 3−6

parameters	3	4	5	6
composition	$C_{77}H_{101}Dy_2\ N_5O_{19}Zn_2$	$C_{77}H_{97}Dy_2\ N_5Ni_2O_{17}$	$C_{78}H_{103}Cl\ La_2N_4Ni_2O_{20}$	$C_{77}H_{97}N_5\ Ni_2O_{17}Tb_2$
formula wt.	1856.37	1807.02	1847.33	1799.86
crystal system	monoclinic	monoclinic	monoclinic	monoclinic
space group	$P2_1/c$	$P2_1/c$	$P2_1/c$	$P2_1/c$
a, Å	12.8187(13)	12.6254(7)	12.5011(5)	12.6371(5)
b, Å	23.343(2)	23.2459(13)	23.4242(10)	23.2036(10)
c, Å	27.448(3)	27.3308(16)	28.2129(12)	27.4871(11)
α, deg	90.00	90.00	90.00	90.00
β, deg	93.054(5)	92.947(2)	92.853(2)	93.003(2)
γ, deg	90.00	90.00	90.00	90.00
V, Å^3	8201.5(14)	8010.7(8)	8251.3(6)	8048.9(6)
ρ_{calc}, Mg m^{-3}	1.503	1.498	1.487	1.485
temp, K	298(2)	298(2)	298(2)	298(2)
λ (Mo K_α), Å	0.71073	0.71073	0.71073	0.71073
Z	4	4	4	4
$F(000)/\ \mu$ mm^{-1}	3768/2.448	3672/2.374	3784/1.566	3664/2.263
$2\theta_{max}$ [deg]	49.82	54.00	50.62	48.54
reflections collected/unique	14236/11121	17403/12597	14939/11403	12946/9966
R_{int}/ GOF on F^2	0.0712/1.361	0.0682/1.404	0.0641/1.322	0.0629/1.547
no. of parameters	962	898	981	897
$R1^a(F_o)$, $wR2^b(F_o)$ (all data)	0.0818	0.0985	0.0861	0.0901
	0.2020	0.2211	0.1970	0.2276
largest diff. peak, deepest hole, e Å^{-3}	1.926, −2.150	2.338, −2.081	1.461, −1.121	1.526, −1.717

$^aR = \sum||F_o| - |F_c||/\sum|F_o|$. $^bwR = [\sum w(F_o^2 - F_c^2)^2/\sum w(F_o^2)^2]^{1/2}$.

$R = \sum||F_o| - |F_c||/\sum|F_o|$, $wR = [\sum w(F_o^2 - F_c^2)^2/\sum w(F_o^2)^2]^{1/2}$, and $S = [\sum[w(F_o^2 - F_c^2)^2]/(n - p)]^{1/2}$. SHELXL-97 was used for both structure solutions and refinements.[19] A summary of the relevant crystallographic data and the final refinement details are given in Table 1. All non-hydrogen atoms were refined anisotropically. The hydrogen atoms were calculated and isotropically fixed in the final refinement [d(C−H) = 0.95 Å, with the isotropic thermal parameter of U_{iso}(H) = 1.2 U_{iso}(C)]. The SMART and SAINT software packages[20] were used for data collection and reduction, respectively. Crystallographic diagrams were drawn using the DIAMOND software package.[21] In compound **4**, C(58), C(59), C(74) carbon atoms and the disordered nitrate ion and methanol solvate were refined isotropically because of the instability of their anisotropic refinements. In compound **6**, C(58), C(59), C(75) carbon atoms and the disordered methanol solvate and nitrate ion were refined isotropically.

RESULTS AND DISCUSSION

Synthesis. A new family of tetranuclear 3d-4f heterometal complexes has been synthesized by a single-pot reaction following the "metal complexes as ligand" approach. The compounds are obtained in good yields by combining $LnX_3{\cdot}6H_2O$ (X = NO_3^- for **3**, **4**, **6**, **7** and ClO_4^- for **5**) with [Zn(HL)(dbm)] (for **3**)/[Ni(HL)(dbm)]·$2CH_3OH$ (for **4**, **5**, **6**, and **7**) in 1:1 mol ratio in methanol in the presence of tetrabutylammonium hydroxide. The adopted strategy for these syntheses is outlined in Scheme 1 in which the precursor complexes [M(HL)(dbm)] (M = Ni^{II}, **1**; Zn^{II}, **2**) are shown as revealed from their crystal structures (Supporting Information, Figures S1 and S2, respectively). These precursor complexes containing the tetradentate N_2O_2 ligand and dibenzoylmethane function here as "metalloligands" to the incoming lanthanide ion to form a 2 × 2 complex in which the metal ions are connected by bridging hydroxido ligands through μ_3- and μ_4-modes as revealed from X-ray crystallography (see later). The nitrogen atoms of the ligand, H_2L, remain coordinated to the Ni^{II}/Zn^{II} ions while the lanthanides are both entrapped in an all

Scheme 1. Syntheses of Complexes 3−7[a]

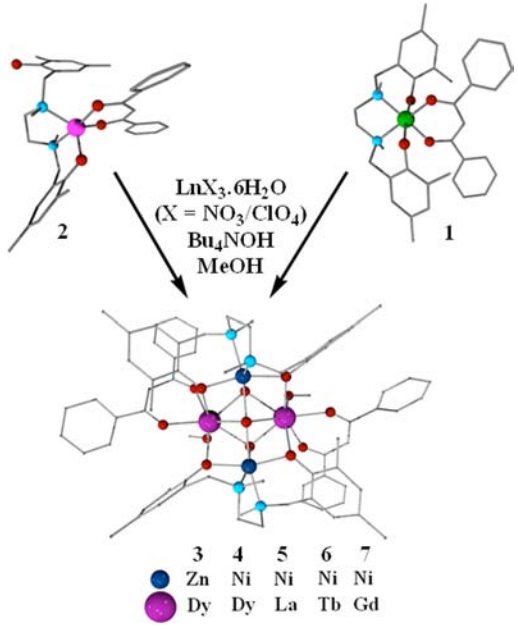

[a]Color codes: sky blue, N; dark red, O; gray, C; green, Ni; pink, Zn.

oxygen O_8 coordination environment which includes a coordinated methanol besides hydroxido- and β-diketonate oxygen atoms. The high thermodynamic stability of this tetranuclear core is possibly the driving force here that enforces one of the hydroxido groups to bridge all the four metal centers in a rare μ_4-type mode. In the literature, several tetranuclear complexes containg M_2Ln_2 (M = Ni, Co, Cu, Fe, Mn) cores have been reported.[22] Some of these cores have butterfly (or defect dicubane) structure,[22a−e] as observed in the present

dx.doi.org/10.1021/ic301138r | Inorg. Chem. 2012, 51, 10211−10221

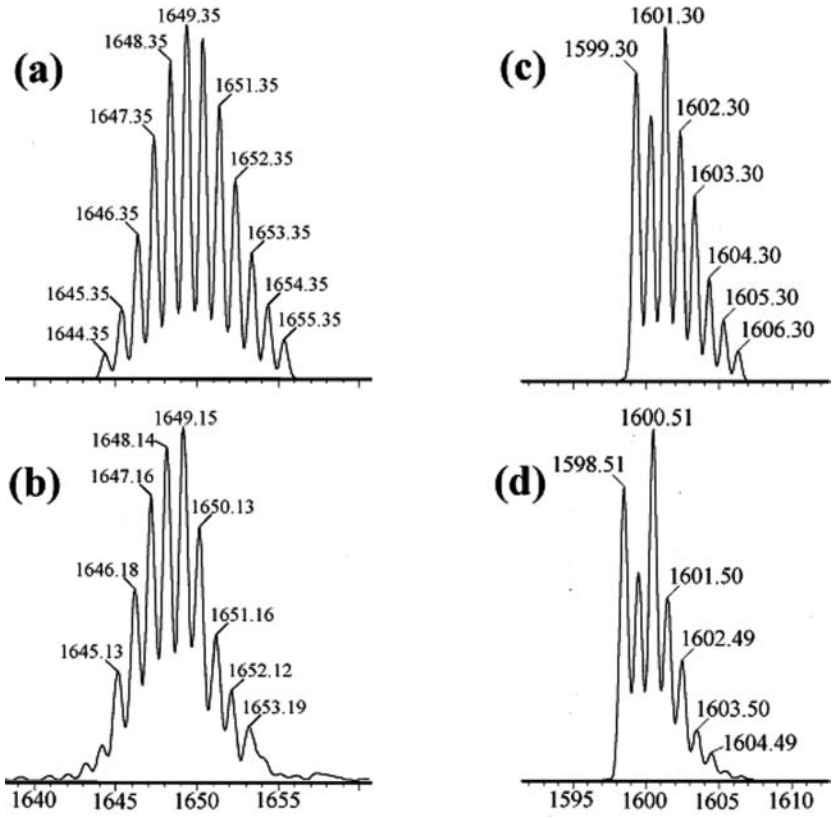

Figure 1. Molecular ion peaks in the ESI mass spectra (positive ion mode) for the complexes **4** and **5** in acetonitrile with (a) and (c) simulated and (b) and (d) observed isotopic distribution patterns, respectively.

series of compounds and established by X-ray diffraction analysis (see later).

IR spectra of the complexes **3**–**7** show all the characteristic bands for the coordinated tetradentate ligand $(L)^{2-}$. One such prominent band appears at about 1255 cm^{-1} due to ν(C–O/phenolate) stretching while for the β-diketonate moiety, the characteristic band due to $\nu_{C=O}$ appears at about 1660 cm^{-1}.[23] For the NO_3^- and ClO_4^- anions, their signature bands, as expected, appear at around 1390 and 1070 cm^{-1}, respectively.[23]

Mass Spectrometry. ESI-MS data (in the positive ion mode) for the complexes **4**–**7** are listed in the Experimental Section. All of these compounds except **3** demonstrate their respective molecular ion peaks due to the $[M\text{-}NO_3\text{-}3CH_3OH]^+$ (for **4**, **6**, and **7**), and $[M\text{-}ClO_4\text{-}4CH_3OH\text{-}H_2O]^+$ (for **5**) ionic species. Figures 1b and 1d display the isotope distribution patterns for the molecular ion peaks for the two representative compounds **4** and **5**, respectively. Corresponding simulation patterns are displayed in Figures 1a and 1c, respectively. The results confirm the integrity of these tetranuclear compounds with the desired heterometal combinations in solution. Spectrum of **3** however did not display the molecular ion peak (Supporting Information, Figure S3) corresponding to the intact molecule. The isotope distribution patterns for the molecular ion peaks of **6** and **7** are also displayed in Supporting Information, Figures S4 and S5, respectively.

Description of Crystal Structures. Single crystal X-ray diffraction analyses have revealed that the cationic parts of the heterometal complexes in **3**–**6** are all isostructural. For the sake of brevity, therefore, a generic description of these structures will be provided considering complex **4** as a representative example. Identical atom-labeling schemes have been adopted for all the structures for easy comparison of their relevant metrical parameters as listed in Table 2. Complex **4** crystallizes in the monoclinic space group $P2_1/c$ with four molecular weight units accommodated in the unit cell. A perspective view of the tetranuclear cationic part of **4** is depicted in Figure 2. The molecular structures and atomic labeling schemes for **3**, **5**, and **6** are displayed in Figures 3, 4, and 5, respectively, which provide confirmatory evidence in support of their grossly identical tetranuclear structures. The asymmetric unit consists of a cationic tetranuclear entity $[Ni_2Dy_2L_2(\mu_3\text{-}OH)_2(\mu_4\text{-}OH)(dbm)_2(MeOH)_2]^+$, a noncoordinated nitrate anion for charge balance, and a methanol molecule as solvent of crystallization. The metal centers of the tetranuclear core are linked by two μ_3-OH^-, one μ_4-OH^-, and four μ-phenoxido oxygen atoms from two deprotonated L^{2-} ligands. Two L^{2-} ligands bridge the Dy^{III} and Ni^{II} centers from opposite sides with Ni^{II} ions occupying the octahedral sites provided by the N_2O_4 donor sets, while the larger Dy^{III} ions take up the eight-coordination sites involving an all oxygen O_8 core, providing a distorted dodecahedral geometry (Figures 6). The coordination sphere around the Ni(1) and Ni(2) centers in this octahedral core are occupied by O(1), N(1), N(2), and O(2) [O(3), N(3), N(4), and O(4) for Ni(2)] donor atoms, all coming from the peripheral tetradentate ligand $(L)^{2-}$, together with O(9) and O(10) atoms [O(9) and O(11)] from the bridging hydroxido ligands. The basal plane around the Ni(1) center is formed by the hydroxido oxygen atoms O(9) and O(10) [O(9) and O(11) for Ni(2)] along with the amino nitrogen atoms N(1) and N(2) [N(3) and N(4)], while the axial positions are occupied by the phenolato oxygen atoms O(1) and O(2) [O(3) and O(4)]. The Ni–N and Ni–O bond lengths are in the normal

dx.doi.org/10.1021/ic301138r | Inorg. Chem. 2012, 51, 10211–10221

Table 2. Selected Bond Distances (Å) and Angles (deg) for 3−6

parameters	**3**; M = Zn; Ln = Dy	**4**; M = Ni; Ln = Dy	**5**; M = Ni; Ln = La	**6**; M = Ni; Ln = Tb
		Bond Distances (Å)		
Ln1−O2	2.315(6)	2.308(5)	2.441(5)	2.324(7)
Ln1−O3	2.328(6)	2.307(5)	2.415(5)	2.322(7)
Ln1−O5	2.296(6)	2.291(6)	2.418(5)	2.342(7)
Ln1−O6	2.341(6)	2.340(6)	2.482(6)	2.374(8)
Ln1−O9	2.519(5)	2.518(5)	2.649(4)	2.554(6)
Ln1−O10	2.359(6)	2.331(5)	2.546(4)	2.434(7)
Ln1−O11	2.440(6)	2.425(5)	2.480(4)	2.360(6)
Ln1−O12	2.392(7)	2.391(7)	2.607(6)	2.412(9)
Ln2−O1	2.327(6)	2.300(5)	2.428(5)	2.335(7)
Ln2−O4	2.311(6)	2.314(5)	2.444(5)	2.325(7)
Ln2−O7	2.306(6)	2.276(6)	2.409(5)	2.288(7)
Ln2−O8	2.330(6)	2.320(6)	2.494(5)	2.344(7)
Ln2−O9	2.530(6)	2.519(5)	2.687(4)	2.529(6)
Ln2−O10	2.433(6)	2.403(5)	2.477(4)	2.348(6)
Ln2−O11	2.345(6)	2.322(5)	2.533(5)	2.425(7)
Ln2−O13	2.415(7)	2.411(7)	2.564(6)	2.431(8)
M1−O1	2.103(5)	2.079(5)	2.070(4)	2.057(6)
M1−O2	2.097(6)	2.059(5)	2.078(4)	2.092(6)
M1−N1	2.167(8)	2.106(8)	2.135(6)	2.142(10)
M1−N2	2.135(7)	2.081(8)	2.088(6)	2.089(9)
M1−O9	2.267(5)	2.174(5)	2.190(4)	2.151(6)
M1−O10	2.100(6)	2.079(6)	2.102(5)	2.075(7)
M2−O3	2.124(5)	2.076(5)	2.080(4)	2.053(6)
M2−O4	2.112(5)	2.043(5)	2.086(4)	2.073(6)
M2−N3	2.173(8)	2.128(8)	2.117(6)	2.081(9)
M2−N4	2.116(8)	2.080(6)	2.100(6)	2.084(9)
M2−O9	2.227(6)	2.144(5)	2.162(4)	2.179(6)
M2−O11	2.094(6)	2.071(6)	2.102(5)	2.098(7)
		Bond Angles (deg)		
O2—Ln1−O3	108.2(2)	106.8(2)	105.10(17)	106.3(2)
O5—Ln1−O6	72.7(2)	73.0(2)	68.82(18)	72.2(3)
O2—Ln1−O10	76.7(2)	76.46(19)	66.45(15)	69.5(2)
O3—Ln1−O10	133.55(19)	132.03(18)	124.54(15)	126.9(2)
O2—Ln1−O11	128.53(19)	127.51(18)	128.02(15)	132.1(2)
O3—Ln1−O11	70.2(2)	69.69(19)	72.84(15)	76.2(2)
O10—Ln1−O11	71.70(19)	71.46(19)	72.97(15)	71.8(2)
O2—Ln1−O9	67.11(19)	66.26(17)	70.18(14)	73.4(2)
O3—Ln1−O9	74.58(18)	73.49(17)	63.98(14)	65.7(2)
O10—Ln1−O9	64.98(19)	64.20(18)	61.81(14)	62.5(2)
O11—Ln1−O9	63.02(18)	62.69(17)	62.52(15)	64.2(2)
O4—Ln2−O1	107.3(2)	107.5(2)	102.87(16)	107.7(2)
O7—Ln2−O8	72.6(2)	72.4(2)	69.32(18)	72.1(3)
O4—Ln2−O11	76.5(2)	75.50(19)	67.56(15)	69.0(2)
O1—Ln2−O11	132.82(19)	132.36(18)	123.96(15)	127.9(2)
O1—Ln2−O10	70.2(2)	69.50(19)	73.03(15)	75.3(2)
O4—Ln2−O10	129.16(19)	127.35(18)	128.56(15)	131.6(2)
O11—Ln2−O10	72.1(2)	72.01(19)	73.25(15)	72.2(2)
O1—Ln2−O9	74.29(18)	74.04(17)	63.60(14)	65.7(2)
O4—Ln2−O9	66.78(19)	65.62(17)	70.29(14)	73.4(2)
O11—Ln2−O9	64.14(19)	64.05(18)	61.33(14)	63.8(2)
O10—Ln2−O9	63.82(18)	63.22(17)	62.11(14)	64.0(2)
O2—M1−O1	159.1(2)	161.7(2)	164.1(2)	163.1(3)
O2—M1−O10	87.5(2)	87.8(2)	81.71(18)	81.3(3)
O10—M1−O1	81.3(2)	80.3(2)	88.79(18)	87.6(3)
O2—M1−N2	90.3(2)	91.1(3)	104.8(2)	104.5(3)
O1—M1−N2	109.4(3)	105.0(3)	89.4(2)	90.2(3)
O10—M1−N2	104.4(3)	102.7(3)	101.0(2)	101.4(4)
O2—M1−N1	101.6(3)	102.1(3)	88.2(2)	88.1(3)
O1—M1−N1	87.4(3)	88.4(2)	100.5(2)	102.0(3)
O10—M1−N1	167.4(3)	168.1(2)	169.66(19)	168.9(3)

dx.doi.org/10.1021/ic301138r | *Inorg. Chem.* 2012, 51, 10211−10221

Table 2. continued

parameters	3; M = Zn; Ln = Dy	4; M = Ni; Ln = Dy	5; M = Ni; Ln = La	6; M = Ni; Ln = Tb
		Bond Angles (deg)		
N2—M1—N1	84.4(3)	84.0(3)	83.8(2)	84.3(4)
O2—M1—O9	75.6(2)	77.2(2)	86.71(17)	87.0(2)
O1—M1—O9	84.4(2)	86.2(2)	78.76(17)	77.8(2)
O10—M1—O9	73.8(2)	74.7(2)	76.91(18)	75.6(3)
N2—M1—O9	165.8(2)	168.0(3)	168.00(19)	167.6(3)
N1—M1—O9	99.9(3)	100.7(3)	100.2(2)	100.9(3)
O11—M2—O4	86.6(2)	87.2(2)	82.75(18)	80.4(3)
O4—M2—O3	159.6(2)	162.4(2)	165.51(19)	162.1(3)
O11—M2—O3	81.1(2)	81.4(2)	88.08(18)	88.2(3)
O4—M2—N4	90.7(2)	90.9(2)	102.9(2)	104.9(3)
O11—M2—N4	104.0(3)	101.5(3)	100.5(2)	102.2(4)
N4—M2—O3	108.0(3)	104.5(2)	89.8(2)	90.8(3)
O4—M2—N3	103.3(2)	102.1(3)	87.1(2)	88.2(3)
O11—M2—N3	167.4(2)	168.9(2)	169.4(2)	168.0(3)
O3—M2—N3	87.2(2)	88.0(3)	101.2(2)	102.0(3)
N4—M2—N3	83.9(3)	84.6(3)	85.0(3)	84.1(4)
O4—M2—O9	75.9(2)	77.6(2)	88.34(17)	86.2(2)
O11—M2—O9	73.7(2)	75.2(2)	77.37(18)	75.5(3)
O3—M2—O9	85.0(2)	86.5(2)	78.69(17)	77.6(2)
N4—M2—O9	166.5(2)	168.1(2)	168.31(19)	168.2(3)
N3—M2—O9	100.9(2)	100.7(3)	99.1(2)	100.3(3)
M2—O9—M1	166.2(3)	167.3(3)	168.4(3)	167.1(4)
M2—O9—Ln1	86.42(19)	86.45(18)	86.30(15)	84.5(2)
M1—O9—Ln1	84.43(18)	84.89(17)	87.14(14)	86.1(2)
M2—O9—Ln2	85.22(18)	85.52(17)	86.02(15)	86.3(2)
M1—O9—Ln2	85.44(18)	86.04(17)	85.08(14)	85.7(2)
Ln1—O9—Ln2	95.7(2)	95.30(18)	95.35(15)	95.1(2)
M1—O2—Ln1	93.7(2)	93.2(2)	95.42(17)	93.7(2)
M1—O1—Ln2	94.6(2)	94.2(2)	94.72(17)	93.1(2)
M2—O3—Ln1	93.9(2)	93.8(2)	94.53(17)	93.6(3)
M2—O4—Ln2	93.6(2)	93.5(2)	94.30(17)	94.4(2)
M1—O10—Ln1	92.3(2)	92.0(2)	91.80(16)	90.9(2)

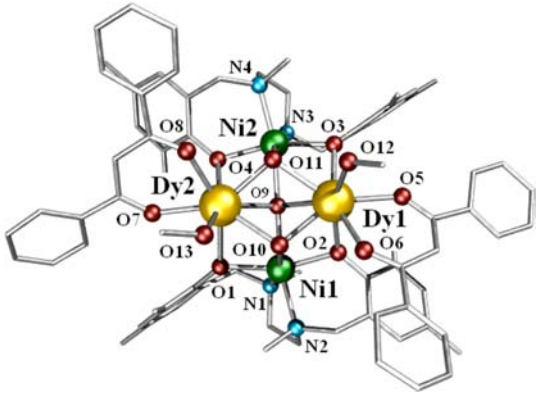

Figure 2. Partially labeled POV-Ray (in ball and stick form) diagram showing the atom labeling scheme for the cationic part in complex **4**.

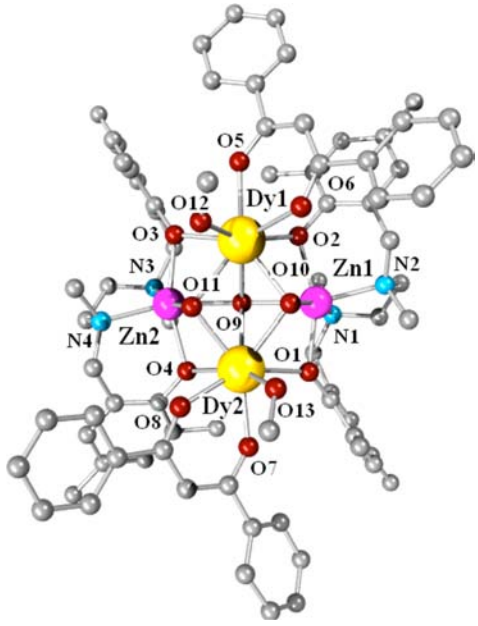

Figure 3. Partially labeled POV-Ray (in ball and stick form) diagram showing atom labeling scheme for the cationic part in complex **3**.

ranges for a NiN_2O_4 chromophore with a distorted octahedral geometry. The trans angles N(1)—Ni(1)—O(10) [168.1(2)°], N(2)—Ni(1)—O(9) [168.0(3)°], N(3)—Ni(2)—O(11) [168.9(2)°], and N(4)—Ni(2)—O(9) [168.1(2)°] are close to linearity, while the remaining two angles, O(1)—Ni(1)—O(2) [161.7(2)°] and O(3)—Ni(2)—O(4) [162.4(2)°], are short of the target. This is most likely due to steric constraints imposed by the bridging phenoxido oxygen atoms O(1), O(2), O(3), and O(4) in this molecule. Both dysprosium ions are eight-coordinated, made up of eight donor oxygen atoms, making distorted dodecahedral geometry around each lanthanide ion.

dx.doi.org/10.1021/ic301138r | *Inorg. Chem.* 2012, 51, 10211—10221

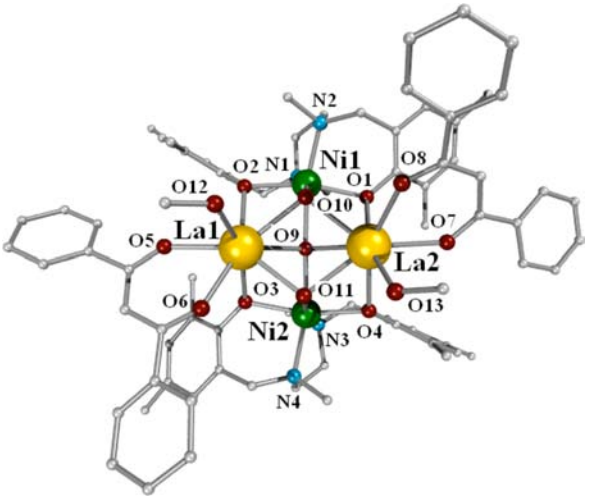

Figure 4. Partially labeled POV-Ray (in ball and stick form) diagram showing atom labeling scheme for the cationic part in complex **5**.

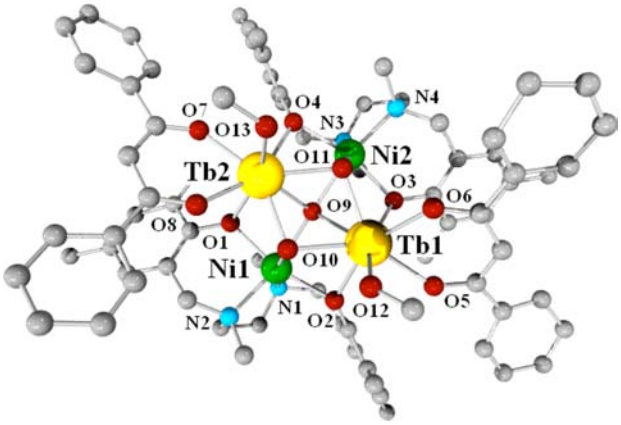

Figure 5. Partially labeled POV-Ray (in ball and stick form) diagram showing atom labeling scheme for the cationic part in complex **6**.

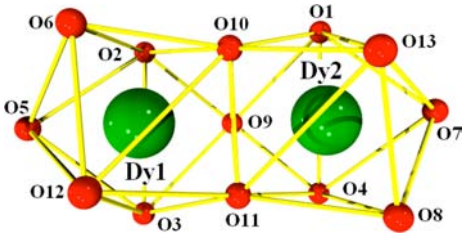

Figure 6. Distorted dodecahedral geometry around Dy1 and Dy2 centers in **4**.

The Dy(1) center is coordinated by five bridging oxygen atoms, namely, O(2), O(3), O(9), O(10), and O(11) [O(1), O(4), O(9), O(10), and O(11) for Dy(2)] playing a crucial role in binding the metal centers, both Ni^{II} and Dy^{III}, together to form a unique butterfly core for a tetranuclear $[Ni_2Ln_2]$ complex. The first two of these are phenoxido oxygen atoms, coming from two tetradentate N_2O_2 ligands, each attached to an adjacent Ni center while the other three are bridging OH^- groups, two of μ_3-type and the third one is in a rare μ_4-type mode (Figures 7). The central oxygen atom O(9) has a distorted square pyramidal geometry with hydrogen atom occupying the axial site and the metal centers occupying the four corners of a rectangular base. The oxygen atom has drifted

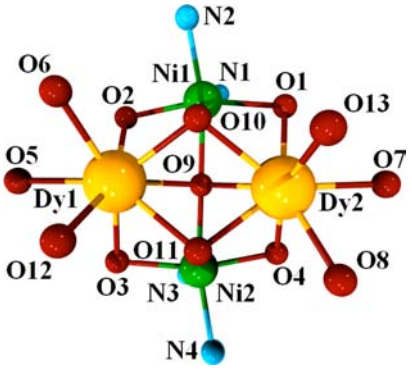

Figure 7. Skeletal view of the cationic part in **4** showing the locations of the donor atoms around the metal centers.

from this plane by 0.969 Å toward the axial hydrogen atom. The remaining three oxygen donors around the Dy^{III} centers are contributed by a chelating dbm^- ligand and a coordinated methanol molecule. The intracluster Ni···Ni and Ln···Ln distances are 4.292 and 3.723 Å, respectively, while the intracluster Ni···Ln separations are very close to each other (~3.178 Å). A salient structural feature of these compounds is that to our knowledge, they represent the first example of nickel-lanthanide tetranuclear complexes with four metal centers connected together by a bridging hydroxido- ligand in a μ_4- mode.

Magnetic Properties. The temperature dependence of magnetic susceptibilities of the isostructural complexes **3**–**7** have been measured on crushed microcrystalline samples over the temperature range 1.8–300 K under an applied direct current (dc) magnetic field of 3000 Oe. The derived χT vs T plots are shown in Figure 8, where χ is the molar magnetic

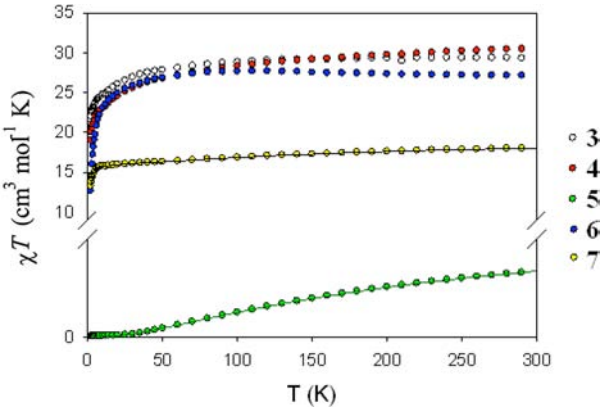

Figure 8. DC magnetic susceptibility data for the series of $M^{II}_2Ln^{III}_2$ complexes as χT vs T plots. The solid lines are the best fitting to the experimental data for **5** and **7**, see text for fitting parameters.

susceptibility per $[M_2Ln_2]$ formula unit. At room temperature, the χT value for **5** is 1.98 cm^3 K mol^{-1}, slightly less than the spin-only value of 2 cm^3 K mol^{-1} expected for two isolated octahedral Ni^{II} ions (S = 1, g = 2.0). With the presence of lanthanum(III) with S = 0 spin state, the magnetic behavior of **5** will give us the information corresponding to the two Ni^{II} ions bridged by a nearly linear oxygen atom. The Ni–O–Ni angle is on average 168°; the coupling should be strongly antiferromagnetic,[24] as it is indeed the case. This is shown by the line with the green dots in Figure 8. The solid line is the

dx.doi.org/10.1021/ic301138r | Inorg. Chem. 2012, 51, 10211–10221

best fitting of the experimental data using an analytical Van Vleck equation for a nickel(II) dimer and the spin-only Hamiltonian $\hat{H} = -2J[S_1 \cdot S_2]$. As temperature decreases, so does the χT value, which is practically zero below 35 K, indicating strong antiferromagnetic coupling between the two Ni^{II} ions. As temperature decreases, the Boltzman population of the isolated $S = 0$ ground state increases. The best fitting has been obtained for $g = 2.02$, $J = -48$ cm^{-1} and a monomeric nickel(II) paramagnetic impurity of 0.2%.

Compound **3** is a Zn_2Dy_2 complex, thus its magnetic properties will reflect the behavior of the Dy_2 unit, since Zn(II) has no unpaired electrons. For this compound, the observed χT value of 29.34 cm^3 K mol^{-1} at 300 K is close to the expected value of 28.3 cm^3 K mol^{-1} for two uncoupled Dy^{III} ions ($^6H_{15/2}$, $S = 5/2$, $L = 5$, $J = 15/2$, and $g = 4/3$).[25] The data for this $Zn^{II}_2Dy^{III}_2$ compound give us an indication of how the lanthanide part in the molecule behaves, without the coupling to the paramagnetic 3d-metal part. In this case, as temperature decreases, the χT product slightly increases, possibly showing some very weak coupling between the two Dy^{III} ions. Because of the strong spin orbit coupling of Dy^{III}, the data cannot be modeled.

For **4** and **6**, the observed χT values of 30.52 and 27.15 cm^3 K mol^{-1} at 300 K are close to the expected values of 30.3 and 26.0 cm^3 K mol^{-1}, respectively for two uncoupled Ln^{III} ions, Dy^{III} and Tb^{III}, (for Dy^{III}: $^6H_{15/2}$, $S = 5/2$, $L = 5$, $J = 15/2$, and $g = 4/3$ and Tb^{III}: $^7F_6$, $S = 3$, $L = 3$, $J = 6$, and $g = 3/2$)[25] and two uncoupled Ni^{II} ions ($S = 1$ and $g = 2$). Interestingly, these two compounds display opposite behavior with the decrease in temperature, the χT product for **4** decreases while that of **6** increases marginally but in both the cases, the χT product reaches a plateau of about 26 cm^3 K mol^{-1} at 50 K and then drop further to the minimum values of about 18 and 13 cm^3 K mol^{-1} at 2 K as indicated by the red and blue dotted lines in Figure 8, indicating the presence of weak- or noninteracting 4f metal ions in these compounds. However, it is difficult to comment on the precise nature of magnetic interactions between the metal ions in these compounds of dysprosium(III) and terbium(III) ions having intrinsic spin−orbit coupling and magnetic anisotropy.[26]

In compound **7** however, the introduction of magnetically isotropic gadolinium(III) ions allows us to estimate the magnetic interactions between Ni···Ni, Gd···Gd, and Ni···Gd centers. This simulation study helps us to understand the magnetic behaviors of other members of this isostructural series containing anisotropic lanthanide ions, whose magnetic properties are much more complicated to understand. For **7**, at room temperature, the χT value of 18.04 cm^3 K mol^{-1} is in good agreement with the expected value of 17.8 cm^3 K mol^{-1} for two uncoupled Gd^{III} ions ($^8S_{7/2}$, $S = 7/2$, and $g = 2.0$) and two noninteracting Ni^{II} ions ($S = 1$ and $g = 2.0$).[25] The χT product remains practically constant down to 10 K and then drops further to a minimum value of 13 cm^3 K mol^{-1} at 2 K as shown by the yellow-dotted line in Figure 8. To gain some information concerning the interactions between these metal ions, an analytical Van Vleck equation can be derived for this complex following the spin exchange Hamiltonian:

$$\hat{H} = -2J_{Ni}(\hat{S}_{Ni1}\cdot\hat{S}_{Ni2}) - 2J_{NiGd}(\hat{S}_{Ni1}\cdot\hat{S}_{Gd1} + \hat{S}_{Ni1}\cdot\hat{S}_{Gd2} + \hat{S}_{Ni2}\cdot\hat{S}_{Gd1} + \hat{S}_{Ni2}\cdot\hat{S}_{Gd2}) - 2J_{Gd}(\hat{S}_{Gd1}\cdot\hat{S}_{Gd2})$$

where the numbering corresponds to that in Scheme 2. The J_{Ni} value was fixed to -50 cm^{-1}, using the value obtained from the

Scheme 2. Representation of the Magnetic Exchanges between the Spin Carriers in 7

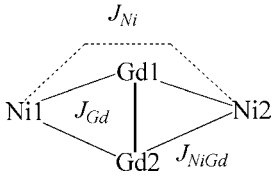

fitting of the susceptibility data of the complex **5**. The best fitting is shown in Figure 8 with a black solid line, and the fitting parameters are $g = 2.1$, $J_{Gd} = -0.02$ cm^{-1} and $J_{NiGd} = -4.65$ cm^{-1} with $J_{Ni} = -50$ cm^{-1}. As expected, the Gd−Gd and the Ni−Gd coupling are extremely weak and similar to reported couplings between 3d metals and lanthanide ions.[27−29] This is further reflected in Figure 9, which shows magnetization vs field

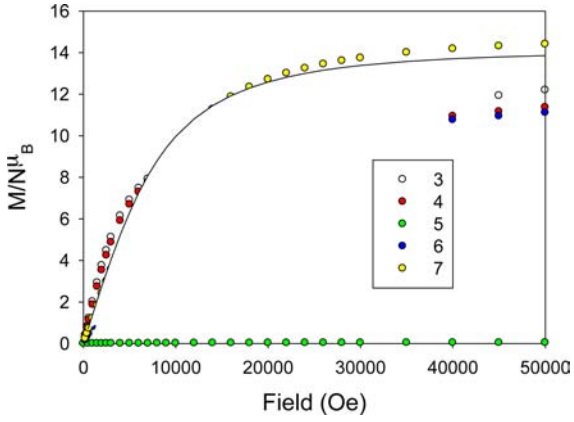

Figure 9. Magnetization vs field plots for **3**−**7** complexes at 2 K. The solid line is the Brillouin function at 2 K for two practically isolated gadolinium(III) ions with $S = 7/2$ and $g = 2.0$.

behavior for these complexes. The data for **7** can be clearly modeled with the Brillouin function for two isolated Gd^{III} ions with $g = 2.0$ and $S = 7/2$. To compare the coupling between lanthanide ions, one can follow the methodology described in the literature,[10n,27,28] in which the data for a La-3d complex is subtracted from the data for the Ln-3d complex of interest, thus obtaining the susceptibility of the paramagnetic Ln part of the complex. To do so, we have subtracted the susceptibility of Ni_2La_2, complex **5**, from the susceptibility of complexes **4**, **6**, and **7**. The results are shown in Figure 10, where one can clearly see how the Gd−Gd and Dy−Dy interaction is extremely weak, and how the Tb−Tb interaction is stronger and ferromagnetic.

To investigate the presence of slow relaxation of the magnetization, ac susceptibility measurements were performed on the complexes **3**, **4**, and **6** as a function of temperature in zero applied dc field and 3.5 Oe oscillating field at frequencies 10−1500 Hz. The $Ni^{II}_2Dy^{III}_2$ (**4**) and $Ni^{II}_2Tb^{III}_2$ (**6**) complexes do not exhibit any slow magnetic relaxation, as has been confirmed by the lack of an out-of-phase ac signal. Interestingly, the tail of an out-of-phase signal at temperatures below 6 K is observed in the case of **3** (Figure 11), indicating the onset of slow magnetization relaxation, which is typical for SMM and single ion magnet (SIM) behavior. Unfortunately, the maxima in the χ'' vs T plots are not reached in the accessible range of frequencies and temperatures of the Squid equipment in use for

dx.doi.org/10.1021/ic301138r | Inorg. Chem. 2012, 51, 10211−10221

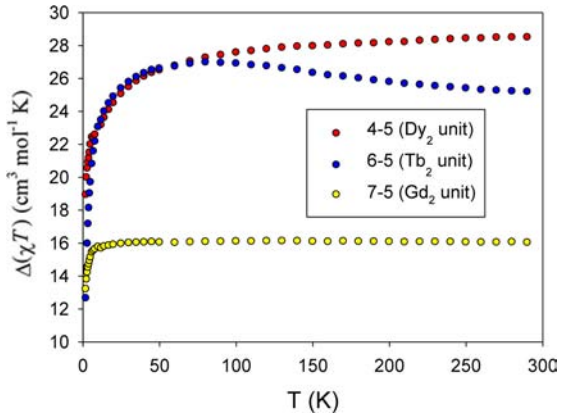

Figure 10. $\Delta(\chi T)$ vs T plots for the complexes **4**, **6**, and **7** showing the variation of susceptibility for the Dy_2, Tb_2, and Gd_2 units, respectively, in the complexes.

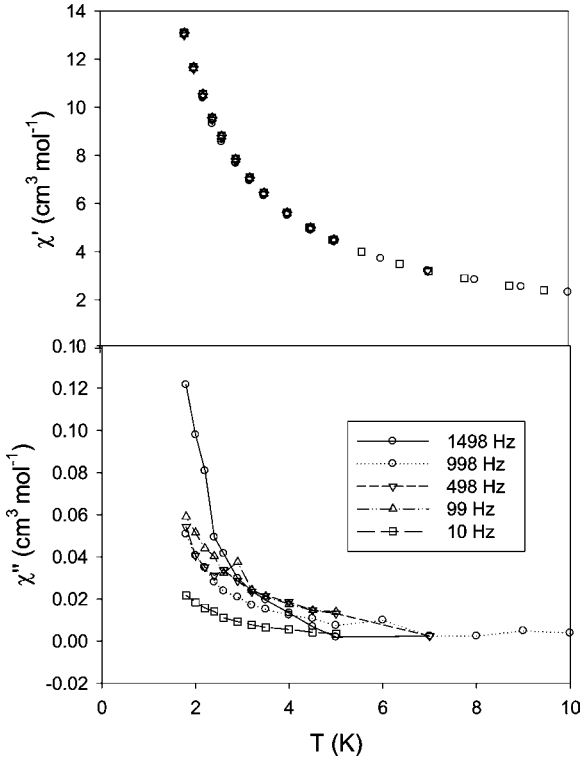

Figure 11. Temperature dependence of the ac magnetic susceptibility for **3** in zero applied dc field and 3.5 Oe oscillating field at frequencies 10−1500 Hz. Top: In-phase component (χ'). Bottom: Out-of-phase component (χ'') below 10 K. As the maximum in the out-of-phase signal is not seen, the in-phase signals at different frequencies still overlap in this temperature regime.

this study. This impedes the determination of the corresponding relaxation time τ.

Disappearance of the out-of-phase ac signal in complex **4** is really surprising considering this molecule to contain Ni^{II} and Dy^{III} ions, both having high single ion anisotropies. In fact the only other antiferromagnetically coupled Ni^{II}−Dy^{III} compound (with a $Ni^{II}_3Dy^{III}$ core) reported in literature[10] did display superparamagnetic behavior of an SMM. Also as reported recently, a defect-dicubane $Ni^{II}_2Dy^{III}_2$ compound as well as some binuclear $Ni^{II}Dy^{II}$ compounds in which the nickel(II) and dysprosium(III) centers are ferromagnetically connected, did show SMM behavior.[10e,f] In compound **4**, where the nickel(II) and dysprosium(III) centers are weakly antiferromagnetically connected, the slow magnetization relaxation becomes faster or is completely quenched because of new relaxation pathways caused by the mixing of the d and f orbitals that are not present when Zn(II) is in the structure instead of Ni(II). In fact in compound **3**, where the diamagnetic Zn^{II} centers are present, its magnetic slow-relaxation behavior possibly originates from the anisotropic Dy^{III} ions,[10c] as is observed in several mono- and polynuclear dysprosium(III) compounds having suitable coordination environments, capable of providing highly anisotropic situations.[30]

CONCLUSIONS

A new family of isostructural heterometal tetranuclear complexes containing a $[Ni^{II}_2Ln^{III}_2]$ core has been synthesized by a single-pot synthesis protocol using $[Ni^{II}(HL)(dbm)]\cdot 2CH_3OH$ as metalloligand. All the four metal centers in these tetranuclear complexes are connected by a bridging hydroxide ligand in a rare μ_4-mode. An extensive magnetic study indicates strong Ni···Ni antiferromagnetic exchange interaction (J_{Ni} = −48 cm^{-1}) in **5**. A moderately weak Ni···Gd (J_{NiGd} = −4.65 cm^{-1}) and a very weak Gd···Gd (J_{Gd} = −0.02 cm^{-1}) exchange interactions, both of antiferromagnetic nature are operative in **7**. The $Zn^{II}_2Dy^{III}_2$ compound (**3**), prepared by an analogous procedure, appears to be the sole member of this series, showing a frequency-dependent out-of-phase signal in ac susceptibility measurement, indicative of slow relaxation of magnetization. The $Ni^{II}_2Dy^{III}_2$ compound (**4**) in which both participating metal ions possess large single ion anisotropy and unpaired electrons, did not show up any slow magnetic relaxation. In these 3d-4f compounds where the metal centers are all antiferromagnetically connected, efficient quantum tunneling of magnetization pathways are effective, and the magnetic relaxation in the $Ni^{II}_2Dy^{III}_2$ compound (**4**) is quenched at the observed temperatures. Thus, it is our conclusion that as observed for many lanthanide complexes that display slow relaxation, this is due to the single-ion effects:[31,32] in fact, the coupling between Ln ions or between Ln ions and 3d metals only provides more efficient tunneling or relaxation pathways, quenching the slow relaxation of the magnetization and results in a nuisance and something to avoid if chemists want to synthesize functional magnets at the molecular level. To conclude, the lanthanide ions have been shown to be quite poor at affording better SMMs; in fact, they are very good SIMs, like Ishikawa's mononuclear complexes,[30b,33] and the development of functional complexes with lanthanide ions should exploit this property.

ASSOCIATED CONTENT

Supporting Information

Partially labeled POV-Ray (in ball and stick form) diagrams of compounds **1** and **2** (Figures S1 and S2), ESI-mass spectra of compounds **3**, **6**, and **7** (Figures S3, S4 and S5), and X-ray crystallographic files in CIF format for compounds **3**−**6**. This material is available free of charge via the Internet at http://pubs.acs.org.

AUTHOR INFORMATION

Corresponding Author

*E-mail: icmc@iacs.res.in.

Notes

The authors declare no competing financial interest.

■ ACKNOWLEDGMENTS

This work was supported by the Council of Scientific and Industrial research (CSIR), New Delhi. Three of the authors, S.M.T.A., M.M., and K.B., also thank the CSIR for the award of research fellowships. The single-crystal X-ray diffraction data were recorded on an instrument supported by DST, New Delhi, as a National Facility at IACS under the IRHPA program. E.C.S. acknowledges financial support form the Spanish Government (Grant CTQ2009-06959 and Ramón y Cajal contract).

■ REFERENCES

(1) (a) Zhao, B.; Chen, X. Y.; Cheng, P.; Liao, D. Z.; Yan, S. P.; Jiang, Z. H. *J. Am. Chem. Soc.* **2004**, *126*, 15394. (b) Blasse, G. *Mater. Chem. Phys.* **1992**, *31*, 3. (c) Sabatini, N.; Guardigli, M.; Lehn, J.-M. *Coord. Chem. Rev.* **1993**, *123*, 201.

(2) (a) Ma, J.-X.; Huang, X.-F.; Song, Y.; Song, X.-Q.; Liu, W.-S. *Inorg. Chem.* **2009**, *48*, 6326. (b) Madalan, A. M.; Bernot, K.; Pointillart, F.; Andruh, M.; Caneschi, A. *Eur. J. Inorg. Chem.* **2007**, 5533.

(3) Sun, W.-B.; Yan, P.-F.; Li, G.-M.; Zhang, J.-W.; Xu, H. *Inorg. Chim. Acta* **2009**, *362*, 1761.

(4) (a) Deng, H.; Shore, S. G. *J. Am. Chem. Soc.* **1991**, *113*, 8538. (b) Deng, H.; Chun, S.; Florian, P.; Grandinetti, P. J.; Sore, S. G. *Inorg. Chem.* **1996**, *35*, 3891.

(5) (a) Sessoli, R.; Powell, A. K. *Coord. Chem. Rev.* **2009**, *253*, 2328. (b) Blake, A. J.; Gould, R. O.; Milne, P. E. Y.; Winpenny, R. E. P. *J. Chem. Soc., Chem. Commun.* **1991**, 1453. (c) Chen, X.-M.; Aubin, S. J. M.; Wu, Y.-L.; Yang, Y.-S.; Mak, T. C. W.; Hendrickson, D. N. *J. Am. Chem. Soc.* **1995**, *116*, 9600. (d) Kong, X.-J.; Long, L.-S.; Zheng, Z.; Huang, R.-B.; Zheng, L.-S. *Acc. Chem. Res.* **2010**, *43*, 201. (e) Mereacre, V.; Baniodeh, A.; Anson, C. E.; Powell, A. K. *J. Am. Chem. Soc.* **2011**, *133*, 15335.

(6) (a) Tasiopoulos, A. J.; Vinslava, A.; Wernsdorfer, W.; Abboud, K. A.; Christou, G. *Angew. Chem., Int. Ed.* **2004**, *43*, 2117. (b) Ako, A. M.; Hewitt, I. J.; Mereacre, V.; Clérac, R.; Wernsdorfer, W.; Anson, C. E.; Powell, A. K. *Angew. Chem., Int. Ed.* **2006**, *45*, 4926. (c) Aromí, G.; Brechin, E. K. *Struct. Bonding (Berlin)* **2006**, *122*, 1. (d) Gatteschi, D.; Sessoli, R.; Villain, J. *Molecular Nanomagnets*; Oxford University Press: Oxford, U.K., 2006. (e) Ako, A. M.; Mereacre, V.; Clérac, R.; Wernsdorfer, W.; Hewitt, I.; Anson, C. E.; Powell, A. K. *Chem. Commun.* **2009**, 544.

(7) (a) Stamatatos, T. C.; Teat, S. J.; Wernsdorfer, W.; Christou, G. *Angew. Chem., Int. Ed.* **2009**, *48*, 521. (b) Langley, S. K.; Moubaraki, B.; Murray, K. S. *Dalton Trans.* **2010**, *39*, 5066. (c) Rigaux, G.; Inglis, R.; Morrison, S.; Prescimone, A.; Cadiou, C.; Evangelisti, M.; Brechin, E. K. *Dalton Trans.* **2011**, *40*, 4797. (d) Papatriantafyllopoulou, C.; Wernsdorfer, W.; Abboud, K. A.; Christou, G. *Inorg. Chem.* **2011**, *50*, 421.

(8) (a) Baniodeh, A.; Hewitt, I. J.; Mereacre, V.; Lan, Y.; Novitchi, G.; Anson, C. E.; Powell, A. K. *Dalton Trans.* **2011**, *40*, 4080. (b) Abbas, G.; Lan, Y.; Mereacre, V.; Wernsdorfer, W.; Clérac, R.; Buth, G.; Sougrati, M. T.; Grandjean, F.; Long, G. J.; Anson, C. E.; Powell, A. K. *Inorg. Chem.* **2009**, *48*, 9345.

(9) Chandrasekhar, V.; Pandian, B. M.; Azhakar, R.; Vittal, J. J.; Clérac, R. *Inorg. Chem.* **2007**, *46*, 5140.

(10) (a) Chandrasekhar, V.; Pandian, B. M.; Boomishankar, R.; Steiner, A.; Vittal, J. J.; Houri, A.; Clérac, R. *Inorg. Chem.* **2008**, *47*, 4918. (b) Mori, F.; Ishida, T.; Nogami, T. *Polyhedron* **2005**, *24*, 2588. (c) Meng, Z.-S.; Guo, F.-S.; Liu, J.-L.; Leng, J.-D.; Tong, M.-L. *Dalton Trans.* **2012**, *41*, 2320. (d) Gao, Y.; Zhao, L.; Xu, X.; Xu, G.-F.; Guo, Y.-N.; Tang, J.; Liu, Z. *Inorg. Chem.* **2011**, *50*, 1304. (e) Georgopoulou, A. N.; Adam, V.; Raptopoulou, C. P.; Psycharis, V.; Ballesteros, R.; Abarca, B.; Boudalis, A. K. *Dalton Trans.* **2010**, *39*, 5020. (f) Colacio, E.; Ruiz-Sanchez, J.; White, F. J.; Brechin, E. K. *Inorg. Chem.* **2011**, *50*, 7268. (g) Colacio, E.; Ruiz, J.; Mota, A. J.; Palacios, M. A.; Cremades, E.; Ruiz, E.; White, F. J.; Euan K. Brechin, E. K. *Inorg. Chem.* **2012**, *51*, 5857. (h) Ke, H.; Zhao, L.; Guo, Y.; Tang, J. *Inorg. Chem.* **2012**, *51*, 2699. (i) Chen, Q.-Y.; Luo, Q.-H.; Zheng, L.-M.; Wang, Z.-L.; Chen, J.-T. *Inorg. Chem.* **2002**, *41*, 605. (j) Costes, J. P.; Vendier, L. *Eur. J. Inorg. Chem.* **2010**, 2768. (k) Yamaguchi, T.; Sunatsuki, Y.; Ishida, H.; Kojima, M.; Akashi, H.; Re, N.; Matsumoto, N.; Pochaba, A.; Mrozinski, J. *Inorg. Chem.* **2008**, *47*, 5736. (l) Pasatoiu, T. D.; Sutter, J.-P.; Madalan, A. M.; Fellah, F. Z. C.; Duhayon, C.; Andruh, M. *Inorg. Chem.* **2011**, *50*, 5890. (m) Costes, J.-P.; Dahan, F.; Dupuis, A.; Laurent, J. P. *Inorg. Chem.* **1997**, *36*, 4284. (n) Cimpoesu, F.; Dahan, F.; Ladeira, S.; Ferbinteanu, M.; Costes, J. -P. *Inorg. Chem.* dx.doi.org/10.1021/ic3001784. (o) Efthymiou, C. G.; Stamatatos, T. C.; Papatriantafyllopoulou, C.; Tasiopoulos, A. J.; Wernsdorfer, W.; Perlepes, S. P.; Christou, G. *Inorg. Chem.* **2010**, *49*, 9737.

(11) (a) Costes, J.-P.; Dahan, F.; Dupuis, A. *Inorg. Chem.* **2000**, *39*, 5994. (b) Osa, S.; Kido, T.; Matsumoto, N.; Re, N.; Pochaba, A.; Mrozinski, J. *J. Am. Chem. Soc.* **2004**, *126*, 420. (c) Sakamoto, M.; Manseki, K.; Ōkawa, H. *Coord. Chem. Rev.* **2001**, *219– 221*, 379. (d) Costes, J.-P.; Dahan, F.; Dupuis, A. *Inorg. Chem.* **2000**, *39*, 165. (e) Andruh, M.; Kahn, O.; Sainton, J.; Dromzee, Y.; Jeannin, S. *Inorg. Chem.* **1993**, *32*, 1623.

(12) (a) Burrow, C. E.; Burchell, T. J.; Lin, P.-H.; Habib, F.; Wernsdorfer, W.; Clérac, R.; Murugesu, M. *Inorg. Chem.* **2009**, *48*, 8051. (b) Yamashita, A.; Watanabe, A.; Akine, S.; Nabeshima, T.; Nakano, M.; Yamamura, T.; Kajiwara, T. *Angew. Chem., Int. Ed.* **2011**, *50*, 4016. (c) Feltham, H. L. C.; Lan, Y.; Klower, F.; Ungur, L.; Chibotaru, L. F.; Powell, A. K.; Brooker, S. *Chem.—Eur. J.* **2011**, *17*, 4362.

(13) (a) Rogez, G.; Rebilly, J. N.; Barra, A. L.; Sorace, L.; Blondin, G.; Kirchner, N.; Duran, M.; van Slageren, J.; Parsons, S.; Ricard, L.; Marvilliers, A.; Mallah, T. *Angew. Chem., Int. Ed.* **2005**, *44*, 1876. (b) Stamatatos, T. C.; Abboud, K. A.; Perlepes, S. P.; Christou, G. *Dalton Trans.* **2007**, 3861. (c) Stamatatos, T. C.; Diamantopoulou, E.; Raptopoulou, C. P.; Psycharis, V.; Escuer, A.; Perlepes, S. P. *Inorg. Chem.* **2007**, *46*, 2350. (d) Aromi, G.; Bouwman, E.; Burzuri, E.; Carbonera, C.; Krzystek, J.; Luis, F.; Schlegel, C.; van Slageren, J.; Tanase, S.; Teat, S. J. *Chem.—Eur. J.* **2008**, *14*, 11158. (e) Meally, S. T.; Karotsis, G.; Brechin, E. K.; Papaefstathiou, G. S.; Dunne, P. W.; McArdle, P.; Jones, L. F. *CrystEngComm* **2010**, *12*, 59.

(14) (a) Benelli, C.; Gatteschi, D. *Chem. Rev.* **2002**, *102*, 2369. (b) Sorace, L.; Benelli, C.; Gatteschi, D. *Chem. Soc. Rev.* **2011**, *40*, 3092.

(15) Mialane, P.; Mallart, A.; Blondin, G.; Nivorojkine, A.; Guilhem, J.; Tchertanova, L.; Cesario, M.; Ravi, N.; Bominaar, E.; Girerd, J.; Munck, E. *Inorg. Chim. Acta* **1997**, *263*, 367.

(16) Perrin, D. D.; Armarego, W. L. F.; Perrin, D. R. *Purification of Laboratory Chemicals*, 2nd ed.; Pergamon: Oxford, U.K., 1980.

(17) *SADABS*, version 2.03; Bruker AXS Inc.: Madison, WI, 2002.

(18) Sheldrick, G. M. *Acta Crystallogr.* **1990**, *46A*, 467.

(19) Sheldrick, G. M. *SHELXL-97, Program for Crystal Structure Refinements*; University of Göttingen: Göttingen, Germany, 1996.

(20) *SAINT*, version 6.02; Bruker AXS Inc.: Madison, WI, 2002.

(21) *DIAMOND, Visual Crystal Structure Information System*, version 3.1; Crystal Impact: Bonn, Germany, 2004.

(22) (a) Mishra, A.; Wernsdorfer, W.; Parsons, S.; Christou, G.; Brechin, E. K. *Chem. Commun.* **2005**, 2086. (b) Murugesu, M.; Mishra, A.; Wernsdorfer, W.; Abboud, K. A.; Christou., G. *Polyhedron* **2006**, *25*, 613. (c) Mondal, K. C.; Kostakis, G. E.; Lan, Y.; Wernsdorfer, W.; Anson, C. E.; Powell, A. K. *Inorg. Chem.* **2011**, *50*, 11604. (d) Papatriantafyllopoulou, C.; Abboud, K. A.; Christou, G. *Inorg. Chem.* **2011**, *50*, 8959. (e) Mereacre, V.; Lan, Y.; Clérac, R.; Ako, A. M.; Hewitt, I. J.; Wernsdorfer, W.; Buth, G.; Anson, C. E.; Powell, A. K. *Inorg. Chem.* **2010**, *49*, 5293. (f) Costes, J. P.; Vendier, L.; Wernsdorfer, W. *Dalton Trans.* **2011**, *40*, 1700. (g) Gómez, V.; Vendier, L.; Corbella, M.; Costes, J.-P. *Inorg. Chem.* **2012**, *51*, 6396. (h) Novitchi, G.; Costes, J.-P.; Tuchagues, J.-P.; Vendier, L.; Wernsdorfer, W. *New J. Chem.* **2008**, *32*, 197. (i) Costes, J.-P.;

Shova, S.; Wernsdorfer, W. *Dalton Trans.* **2008**, 1843. (j) Gomez, V.; Vendier, L.; Corbella, M.; Costes, J. P. *Eur. J. Inorg. Chem.* **2011**, 2653. (k) Hamamatsu, T.; Yabe, K.; Towatari, M.; Osa, S.; Matsumoto, N.; Re, N.; Pochaba, A.; Mrozinski, J.; Gallani, J.-L.; Barla, A.; Imperia, P.; Paulsen, C.; Kappler, J.-P. *Inorg. Chem.* **2007**, *46*, 4458.
(23) Nakamoto, K. *Infrared and Raman Spectra of Inorganic and Coordination Compounds*, 3rd ed.; Wiley-Interscience: New York, 1978.
(24) Palacios, M. A.; Mota, A. J.; Perea-Buceta, J. E.; White, F. J.; Brechin, E. K.; Colacio, E. *Inorg. Chem.* **2010**, *49*, 10156.
(25) Kahn, O. *Molecular Magnetism*; VCH Publ. Inc.: New York, 1993.
(26) Zhao, X. Q.; Lan, Y. H.; Zhao, B.; Cheng, P.; Anson, C. E.; Powell, A. K. *Dalton Trans.* **2010**, *39*, 4911.
(27) Estrader, M.; Ribas, J.; Tangoulis, V.; Solans, X.; Font-Bardía, M.; Maestro, M.; Diaz., C. *Inorg. Chem.* **2006**, *45*, 8239.
(28) Figuerola, A.; Diaz, C.; Ribas, J.; Tangoulis, V.; Sangregorio, C.; Gatteschi, D.; Maestro, M.; Mahía., J. *Inorg. Chem.* **2003**, *42*, 5274.
(29) Costes, J.-P.; Auchel, M.; Dahan, F.; Peyrou, V.; Shova, S.; Wernsdorfer, W. *Inorg. Chem.* **2006**, *45*, 1924.
(30) (a) Nayak, S.; Roubeau, O.; Teat, S. J.; Beavers, C. M.; Gamez, P.; Reedijk, J. *Inorg. Chem.* **2010**, *49*, 216. (b) Ishikawa, N.; Sugita, M.; Wernsdorfer, W. *Angew. Chem., Int. Ed.* **2005**, *44*, 2931. (c) Peng, J.-B.; Kong, X.-J.; Ren, Y.-P.; Long, L.-S.; Huang, R.-B.; Zheng, L.-S. *Inorg. Chem.* **2012**, *51*, 2186.
(31) Liu, C.-S.; Du, M.; Carolina Sañudo, E.; Echeverria, J.; Hu, M.; Zhang, Q.; Zhou, L.-M.; Fang, S.-M. *Dalton Trans.* **2011**, *40*, 9366.
(32) Guo, Y.-N.; Xu, G.-F.; Gamez, P.; Zhao, L.; Lin, S.-Y.; Deng, R.; Tang, J.; Zhang, H.-J. *J. Am. Chem. Soc.* **2010**, *132*, 8538.
(33) Ishikawa, N.; Sugita, M.; Ishikawa, T.; Koshihara, S.; Kaizu, Y. *J. Am. Chem. Soc.* **2003**, *125*, 86.